



# UAHOI: Uncertainty-aware Robust Interaction Learning for HOI Detection

Mu Chen<sup>a</sup>, Minghan Chen<sup>a</sup>, Yi Yang<sup>b,\*\*</sup>

<sup>a</sup>Australian Artificial Intelligence Institute, Faculty of Engineering and Information Technology, University of Technology Sydney, NSW, Australia

<sup>b</sup>School of Computer Science, Zhejiang University, Zhejiang, China

## ABSTRACT

This paper focuses on Human-Object Interaction (HOI) detection, addressing the challenge of identifying and understanding the interactions between humans and objects within a given image or video frame. Spearheaded by Detection Transformer (DETR), recent developments lead to significant improvements by replacing traditional region proposals by a set of learnable queries. However, despite the powerful representation capabilities provided by Transformers, existing Human-Object Interaction (HOI) detection methods still yield low confidence levels when dealing with complex interactions and are prone to overlooking interactive actions. To address these issues, we propose a novel approach UAHOI, Uncertainty-aware Robust Human-Object Interaction Learning that explicitly estimates prediction uncertainty during the training process to refine both detection and interaction predictions. Our model not only predicts the HOI triplets but also quantifies the uncertainty of these predictions. Specifically, we model this uncertainty through the variance of predictions and incorporate it into the optimization objective, allowing the model to adaptively adjust its confidence threshold based on prediction variance. This integration helps in mitigating the adverse effects of incorrect or ambiguous predictions that are common in traditional methods without any hand-designed components, serving as an automatic confidence threshold. Our method is flexible to existing HOI detection methods and demonstrates improved accuracy. We evaluate UAHOI on two standard benchmarks in the field: V-COCO and HICO-DET, which represent challenging scenarios for HOI detection. Through extensive experiments, we demonstrate that UAHOI achieves significant improvements over existing state-of-the-art methods, enhancing both the accuracy and robustness of HOI detection.

© 2024 Elsevier Ltd. All rights reserved.

## 1. Introduction

Human-Object Interaction Detection (HOI Detection) aims to localize and recognize HOI triplets in the format of <human, verb, object> from static images (Ni et al., 2023; Leonardi et al., 2024). This field stems from the detection of objects to include their relationships, prompting a deeper understanding on high-level semantic comprehension. HOI Detection has attracted considerable attention for its great potential in numerous high-level visual understanding tasks, including video question answering (Wu et al., 2017), video captioning (Rao et al., 2024; Nian et al., 2017), activity recognition (Ozbulak et al., 2021), and syntia-to-reality translation (Chen et al., 2023a).

Traditional methods (Zhou et al., 2021, 2020; Zhang et al., 2021b; Gkioxari et al., 2018) typically adopt either two-stage or one-stage pipeline, where the former detects instances first and then enumerates human-object pairs to identify their interactions, and the latter attempts to do both simultaneously. However, these methods struggle with modeling the complex, long-range dependencies between humans and objects due to the localized nature of convolutional operations—a limitation that transformer-based methods address by capturing intricate interrelations across entire scenes. Recent advancements (Li et al., 2023c; Chen et al., 2021; Kim et al., 2021; Tamura et al., 2021) have predominantly embraced the encoder-decoder framework pioneered by detection transformers (DETR) (Carion et al., 2020), initializing learnable queries randomly, and subsequently decode the object queries into detailed triplets of human-object interactions. These methods offer enhanced accuracy by capturing global contexts and intricate interrelations,

\*\*Corresponding author: Yi Yang  
e-mail: [yangyics@zju.edu.cn](mailto:yangyics@zju.edu.cn) (Yi Yang)

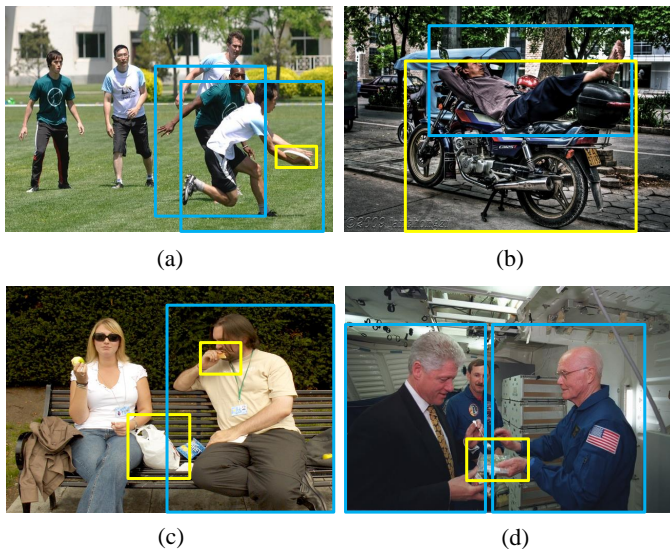


Fig. 1. Common challenges of current HOI Detection methods in complex scenes. The human/object bounding boxes are shown in blue/yellow.

and simplify the architecture by eliminating the need for extra hand-designed components.

Despite the notable advances, several challenges still persist. As shown in Fig 1, **firstly**, among the wide range of predicates, some interactions may not be directly manifested through visual signals, often involving subtle movements and non-physical connections. For example, the interaction looking in a certain direction in (c) may easily be overlooked. And a man lying on a mortobike could be easily recognized as a man riding a mortobike (b). **Secondly**, in a multi-human scene, a person who may be imagining or planning to interact with an object without yet taking any action can easily be mistaken for having already performed the action, such as the unselected background individuals in images (a) and (d). **Thirdly**, the same type of interaction can appear very differently in different contexts. For instance, the action of “grabbing” can vary significantly when interacting with different objects, depending on the object’s size, shape, weight, and other characteristics. In such complex scenarios, current models typically assign lower confidence to interactions, which affect the performance.

To address these issues, conventional two-stage methods involves assistance from extra communication signal (Shen et al., 2018; Li et al., 2023b; Liang et al., 2023; Fan et al., 2019; Wang et al., 2019), and language (Xu et al., 2019; Liu et al., 2020), but the models still tend to focus on inaccurate regions. More recent approaches independently process instance detection and interaction classification using two separate decoders, which operate either in parallel (Zhou et al., 2022) or cascaded (Zhang et al., 2021a; Chen et al., 2021) mode. For example, Zhang et al. (2021a) applied two cascade decoders, one for generating human-object pairs and another for dedicated interaction classification of each pair, which helps the model to determine which regions inside a scene to concentrate on. Taking a step further, Unary (Zhang et al., 2022) separately encodes human and object instances, enhancing the output features with additional transformer layers for more accurate HOI classification. Zhou et al. (2022) disentangle both encoder and

decoder to enhance the learning process for two distinct sub-tasks: identifying human-object instances and accurately classifying interactions, which necessitates learning representations attentive to varied regions. While the disentanglement of sub-tasks allows individual modules to concentrate on their specific tasks, thereby boosting overall performance, these methods often require additional heuristic thresholding when deciding which interactions to retain. For simple interactions, it is relatively easy to obtain good interaction predictions with high confidence scores in their predicted categories. However, for more complex interactions, confidence scores may be lower. In such cases, finding a suitable threshold manually to disregard low-confidence predictions could lead to overlooking correct interactions, representing a persistent challenge in HOI detection. Specifically, determining the optimal threshold value is challenging across different categories, and estimating a value in advance is more complex. For overt interactions like “riding,” where a person is physically mounted on an object such as a bicycle or horse, confidence scores are typically high. In contrast, subtle interactions like “reading,” characterized by the presence of a book and the direction of a person’s gaze, often yield lower overall confidence scores. A high threshold in such cases might cause the model to ignore these interactions.

We propose a novel method UAHOI, Uncertainty-aware Robust Human-Object Interaction Learning that utilizes uncertainty estimation to dynamically adjust the threshold for interaction predictions in the HOI detection task. This approach integrates uncertainty modeling to refine the decision-making process, enabling the model to adjust its confidence thresholds based on the predicted uncertainty associated with each interaction. Specifically, we utilize the variance in predictions as a measure of uncertainty for both human/object bounding boxes and interaction, which reflects the model’s confidence in their outputs. The variance is directly incorporated into our optimization target, enhancing the accuracy of bounding box predictions and ensuring that significant interactions are not overlooked due to artificially low confidence thresholds. Such adaptive handling of complex interactions increases the robustness of HOI detection models. UAHOI handles complex interactions in an adaptive manner, enhancing the accuracy of the bounding box predictions and preventing important interactions from being overlooked due to artificially low confidence thresholds, thereby increasing the robustness of HOI Detection model. We conducted a comprehensive evaluation on two standard human-object interaction datasets HICO-DET (Chao et al., 2018) and V-COCO (Gupta and Malik, 2015), and our experiments demonstrate a significant improvement over the existing state-of-the-art methods. Specifically, UAHOI achieved 34.19 mAP on HICO-DET and 62.6 mAP on V-COCO.

## 2. Related Works

### 2.1. Traditional HOI Detection

Human-Object Interaction (HOI) detection provides numerous high-level intricate relationships between humans and objects, gradually serving as the foundation of many computer vision applications (Wang et al., 2024; Chen et al., 2023b,

2024b,a). Traditional Human-Object Interaction (HOI) detection methods can typically be divided into two categories: two-stage methods (Qi et al., 2018; Gupta et al., 2019; Wan et al., 2019; Xu et al., 2019; Zhou and Chi, 2019; Li et al., 2019; Ullutan et al., 2020; Wang et al., 2020a; Gao et al., 2020; Hou et al., 2020; Li et al., 2020b; Kim et al., 2020b; Li et al., 2020a) and one-stage methods (Kim et al., 2020a; Liao et al., 2020; Wang et al., 2020b; Fang et al., 2021). Two-stage HOI detection methods rely on an off-the-shelf object detector to extract bounding boxes and class labels for humans and objects in the first stage. In the second stage, they model interactions for each human-object pair via a multi-stream network. For example, Qi et al. (2018) propose leveraging the Graph Parsing Neural Network (GPNN) to incorporate structural knowledge into HOI detection. Similarly, Gupta et al. (2019) introduces a streamlined factorized model that utilizes insights from pre-trained object detectors. Subsequent research often involves integrating additional contextual and relational information to enhance performance further. However, two-stage methods find it challenging to identify human-object pairs among a large number of permutations and heavily rely on the detection results, suffering from low efficiency and effectiveness. (Liu et al., 2020; Zhou et al., 2020; Zhang et al., 2021b; Gkioxari et al., 2018; Zhou et al., 2021). By introducing anchor points to associate humans and objects, single-stage methods detect pairs likely to interact and their interactions simultaneously. This approach, which handles instance detection and interaction point prediction branches in parallel, has made impressive progress in HOI detection. For instance, Kim et al. (2020a) utilizes a union-level detector to directly capture the region of interaction, enhancing focus on interaction-specific areas. Meanwhile, Liao et al. (2020) employs point detection branches that concurrently predict points for both the human/object and their interactions. This method not only implicitly provides context but also offers regularization for the detection of humans and objects, improving overall accuracy and context relevance. However, these one-stage methods still fall short in striking an appropriate balance in multi-task learning and modeling long-range contextual information.

## 2.2. End-to-End HOI Detection

Inspired by DETR (Carion et al., 2020), recent work (Chen et al., 2021; Kim et al., 2021; Tamura et al., 2021; Zou et al., 2021; Zhang et al., 2021a; Kim et al., 2022; Zhang et al., 2022; Zhou et al., 2022; Liao et al., 2022; Liu et al., 2022; Yuan et al., 2022a; Zhong et al., 2022) modify HOI as a set-prediction problem by generating a set of HOI triplets. Early approaches (Tamura et al., 2021; Zou et al., 2021) simply migrated the Transformer decoder to HOI tasks, using a single decoder to couple human-object detection and interaction classification, achieving end-to-end training. Tamura et al. (2021) replaces manually defined location-of-interest with a transformer-based feature extractor, enhancing feature representation capabilities. Zou et al. (2021) addresses HOI detection using an end-to-end approach, which eliminates the reliance on hand-designed components, streamlining the detection process. However, due to the significant differences between the

two tasks, learning a unified instance-interaction representation proved challenging. Therefore, subsequent works (Kim et al., 2021; Zhang et al., 2021a; Chen et al., 2021) gradually shifted towards using separate decoders for instance prediction and interaction prediction, allowing the model to fully focus on the differences between instance and interaction prediction areas. To further enhance performance, other methods have introduced language (Yuan et al., 2022b; Cao et al., 2023) and logic-reasoning (Li et al., 2023c) to explore the relationships between humans, objects, and their interactions more deeply. Moreover, scene graph generation (SGG) is another high-level semantic understanding task closely related to HOI detection, which is advanced with the help of techniques such as noisy label correction (Li et al., 2024), LLMs (Li et al., 2023d) and compositional augmentation (Li et al., 2023a). Both HOI Detection and SGG aim to capture and understand complex relationships between objects within a scene, but scene graph generation focuses on identifying objects and their pairwise relationships to create a structured graph representation, while HOI detection specifically targets interactions between humans and objects. Our method is built on a disentangled network framework that separately handles human-object detection and interaction classification tasks.

## 2.3. Uncertainty Estimation

Our work is closely related to Uncertainty Estimation techniques (Frankle et al., 2020). The study of uncertainty estimation within deep learning frameworks is garnering considerable attention. Existing works have explored the uncertainty estimation from different aspects, such as Bayesian approaches (Sensoy et al., 2018; Amini et al., 2020; Gal and Ghahramani, 2016; Gal et al., 2017) and deep ensemble techniques (Lakshminarayanan et al., 2017; Vyas et al., 2018). Bayesian approaches adopt bayesian theory to predict the uncertainty of the neural networks. Among them, Gal and Ghahramani (2016) and Gal et al. (2017) leverage dropout to obtain probability distribution on network parameters, often come with a high computational cost and complexity. Ensemble methods aggregate predictions from multiple networks to estimate uncertainty, providing a balance between computational efficiency and reliability. Uncertainty estimation technologies make great progress in computer vision tasks such as semantic segmentation (Zheng and Yang, 2021; Lu et al., 2023; Fleuret et al., 2021) and object detection (Liu et al., 2016; Miller et al., 2018, 2019), but are less explored for HOI detection. In this work, we integrate uncertainty estimation into HOI detection by modeling bounding box coordinates (left, right, top, bottom) as Gaussian-distributed random variables and using dropout not only for regularization but also to estimate variance in interaction predictions. This allows us to embed uncertainty directly into the learning process, enhancing both the robustness and adaptability of our detection systems. Furthermore, we introduce an Uncertainty-Aware Loss Function and implement Regularization of Interaction Uncertainty as an automatic thresholding mechanism, demonstrating an effective approach to improving HOI detection through advanced uncertainty modeling techniques.

### 3. Methods

#### 3.1. Preliminary: Vanilla Transformer-based HOI Detection

Since DETR (Carion et al., 2020), object detection has been investigated as a set prediction problem. DETR employs a transformer encoder-decoder architecture to transform  $N$  positional encodings into  $N$  predictions, encompassing both object class and bounding box coordinates. Similar to object detection, recent advancements (Chen et al., 2021; Kim et al., 2021; Tamura et al., 2021; Zou et al., 2021; Zhang et al., 2021a; Kim et al., 2022; Zhang et al., 2022; Zhou et al., 2022; Liao et al., 2022; Liu et al., 2022; Yuan et al., 2022a; Zhong et al., 2022) have adeptly harnessed the Encoder-Decoder framework, integrating the Transformer architecture to better capture complex dependencies between humans and objects. This integration significantly enhances model precision and deepens understanding of interactions within a scene (Kim et al., 2021; Zou et al., 2021). In our approach, as is shown in Fig 2, we implement an encoder-decoder structure with a shared encoder alongside two parallel decoders: one for instance localization and another for interaction recognition. This design helps to eliminate the issue of redundant predictions. (Kim et al., 2021). In detail, the feature  $\mathbf{f} \in \mathbb{R}^{D \times H \times W}$  is extracted from the input image  $\mathbf{x}$  via a CNN backbone, where  $H$  and  $W$  are the size of the input image, and  $D$  is the number of channel. Combined with positional embedding  $p$ , the feature  $\mathbf{f}$  containing semantic concepts is flattened to construct a sequence of length  $H \times W$  and then fed into the image encoder. We adopt ResNet as our backbone. Each image encoder layer consists of a multi-head self-attention (MHSA) module and a feed-forward network, which refine the feature representation sequentially. After processing by image encoder, the resulting encoded features, denoted as  $\mathbf{f}_{en} \in \mathbb{R}^{D' \times H' \times W'}$ , are split and fed to the instance localization decoder and interaction recognition decoder. The instance localization decoder identifies and localizes objects within the scene, and the interaction recognition decoder analyzes the interaction between detected objects and humans, aiming to understand their mutual interactions. Object queries  $\mathbf{Q}_{obj} = \{\mathbf{q}_i \mid \mathbf{q}_i \in \mathbb{R}^d\}_{i=1}^H$  and Interaction queries  $\mathbf{Q}_{inter} = \{\mathbf{q}_i \mid \mathbf{q}_i \in \mathbb{R}^d\}_{i=1}^H$  are initialized randomly, and then learnt via cross-attention layers.  $H$  is the number of queries and  $d$  is the query dimension. The decoding process for localization and interaction recognition could be formulated by:

$$\mathbf{L} = \text{Decoder}_{loc}(\mathbf{f}_{en}, \mathbf{Q}_{obj}) \in \mathbb{R}^{H \times 4}, \quad (1)$$

$$\mathbf{I} = \text{Decoder}_{inter}(\mathbf{f}_{en}, \mathbf{Q}_{inter}) \in \mathbb{R}^{H \times C}. \quad (2)$$

where  $\mathbf{Q}_{obj}$  and  $\mathbf{Q}_{inter}$  are sets of initialized queries for object detection and interaction recognition, respectively, refined through cross-attention mechanism.

With the learned HOI queries, the HOI pair could be decoded by several MLP branches. Specifically, we adopt three MLP branches designed to output the confidence levels for the human, object, and their interaction, respectively, each employing a softmax function to ensure probabilistic outputs. The addition of these branches allows for a more granular understanding of the HOI dynamics by providing individual confidence

scores that reflect the certainty of each element’s involvement in the interaction. The output embedding is then decoded into specific HOI instance via several multiple Multi-Layer Perceptron (MLP) layers. In detail, three separate MLP branches are designed to predict the confidence levels for the human, object, and interaction, respectively. Each branch employs a softmax function to generate probabilistic outputs. The human and object branches are denoted by orange color in Figure 2. For human branch, two values with confidence are outputted to indicate the likelihoods of foreground and background presence. Regarding object and interaction branches, the output scores including all categories of objects or actions and another one category for the background. UAHOI adopts two Fully Feed-Forward Networks (FFN) layers to predict the bounding boxes of the human and the object. The bounding box consists of four values to represent each coordinate for precise localization within the visual scene.

#### 3.2. Uncertainty-aware Instance Localization

Firstly, when estimating localization uncertainty, we consider the bounding boxes for both humans, denoted by  $C_{human} \in (l_h, r_h, t_h, b_h)$  and objects, represented as  $C_{object} \in (l_o, r_o, t_o, b_o)$ . This representation allows us to explore inherent uncertainty in the prediction of bounding box coordinates, which is particularly useful in complex scenes where occlusion or interaction may obscure part of the subjects. We employ a dedicated network to compute the standard deviations of these distributions, providing a measurable and quantifiable uncertainty which enhances the precision in object boundary detection. This methodology not only improves accuracy but also increases the reliability of localizations by effectively capturing and quantifying the inherent uncertainties associated with positional offsets. To accurately delineate the object’s boundary, it is essential to account for the four directional offsets of the human/object bounding box. Adopting the framework outlined by (Lee et al., 2022), we implement an uncertainty estimation network tailored to assess the localization uncertainty derived from these regressed box offsets  $(l, r, t, b)$ , defined as Gaussian distributions:

$$l \sim \mathcal{N}(\mu_l, \sigma_l^2), \quad (3)$$

$$r \sim \mathcal{N}(\mu_r, \sigma_r^2), \quad (4)$$

$$t \sim \mathcal{N}(\mu_t, \sigma_t^2), \quad (5)$$

$$b \sim \mathcal{N}(\mu_b, \sigma_b^2). \quad (6)$$

Here,  $\mu$  and  $\sigma^2$  signify the mean and variance of the offsets, respectively. To determine these parameters accurately, we deploy a neural network featuring a dual-head architecture. One head predicts the mean values while the other calculates the logarithm of the variance as *uncertainty*, naming  $Var_{box}$ , ensuring that the variance  $\sigma_{box}$  is always positive:

$$\mu_{box} = \text{MLP}_{\mu}(\mathbf{f}_{en}), \quad (7)$$

$$\sigma_{box}^2 = \log(1 + \exp(\text{MLP}_{\sigma}(\mathbf{f}_{en}))). \quad (8)$$

Further, Lee et al. (2022) introduce a Negative Power Log-Likelihood Loss, which is reformulated to achieve an uncertainty loss. This uncertainty loss compels the network to output

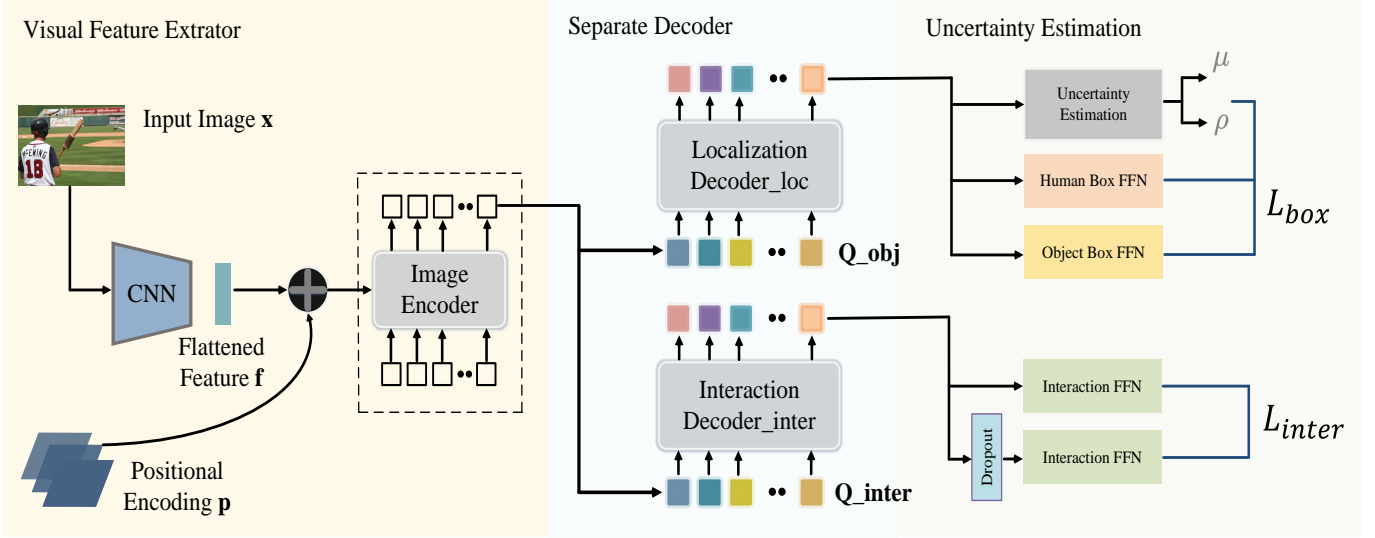


Fig. 2. Overall framework of our UAHOI. UAHOI consists of three components: Visual Feature Extractor, Parallel Decoder and Uncertainty Estimation module. Visual features are firstly extracted by CNN and shared Transformer Encoder. Then, the Localization Decoder and Interaction Decoder run in parallel to extract human/object bounding boxes and interaction class. Lastly, the proposed Uncertainty-aware Instance Localization and Interaction Refinement modules are used to perform uncertainty regularization.

a higher uncertainty value when the coordinate predictions from the regression branch are off-target:

$$L_{box} = - \sum_{c \in \{l, r, t, b\}} IoU \cdot \log P_{\Theta}(C | \mu_c, \sigma_c^2). \quad (9)$$

This equation emphasizes the integration of the Intersection over Union (IoU) as a scaling factor, where IoU measures the overlap between the predicted and actual bounding boxes, enhancing the training focus on precision. The probability density function  $P_{\Theta}$ , parameterized by network parameters  $\Theta$ , plays a crucial role in adjusting the model’s certainty regarding the predicted localizations, thus pushing the boundaries of accuracy in object detection in highly dynamic and unpredictable scenes.

### 3.3. Uncertainty-aware Interaction Refinement

Secondly, to refine the interaction, we model the uncertainty of the interaction classification via the prediction variance. Typically, models tend to make less accurate predictions in complex interaction areas. By modeling uncertainty, we are able to quantitatively calculate this uncertainty. Specifically, if there is a significant difference between predictions made with and without dropout, the variance will be high. This reflects the model’s uncertainty in predicting interactions. Following previous works (Srivastava et al., 2014), we add structured noise to the interaction feature representation via dropout. We denote  $\hat{y}^i = f(x; \hat{\theta}_i)$  and  $y = f(x; \theta)$  as the interaction representation with/without dropout. Following recent works in the field of uncertainty estimation (Zheng and Yang, 2021), we predict the interaction variance *uncertainty*  $Var_{inter}$  as the KL divergence between the two representation:

$$D_{kl} = \mathbb{E} \left[ y \log \left( \frac{y}{\hat{y}^i} \right) \right]. \quad (10)$$

Following (Kendall and Gal, 2017; Zheng and Yang, 2021), we regularize the interaction variance by minimizing the predic-

tion bias, thus enabling the learning from inaccurate interaction. The objective could be formulated as:

$$L_{inter} = \mathbb{E} [\exp \{-D_{kl}\} L_{ce} + D_{kl}]. \quad (11)$$

The final loss to be minimized consists of four parts:

$$L_{total} = L_{loc}^h + L_{loc}^o + \lambda_o L_{box} + \lambda_a L_{inter}. \quad (12)$$

Here,  $\lambda_1$  and  $\lambda_2$  are the weights of two uncertainty losses,  $L_{loc}^h$  and  $L_{loc}^o$  are computed by box regression loss. In this situation, during the optimization process, the variance of both bounding boxes and the interaction will be minimized.

### 3.4. Implementation Details

**Network Architecture.** To ensure a fair comparison with existing works (Kim et al., 2021; Zou et al., 2021; Chen et al., 2021), we adopt ResNet-50 as our backbone, followed by a six-layer transformer encoder as our visual feature extractor. Both the Localization and Interaction Decoder consist of four Transformer decoder layers.

**Training.** During training, all of the transformer layer weights are initialized with Xavier init (Glorot and Bengio, 2010). UAHOI is optimized by AdamW (Loshchilov and Hutter, 2017) and we set the initial learning rate of both encoder and decoder to  $10^{-4}$  and weight decay to  $10^{-4}$ . The weight coefficients  $\lambda_o$  and  $\lambda_a$  are set to 1 and 1. To fairly compare with existing methods, the Backbone, Image Encoder and both Localization and Interaction Decoder are pretrained in MS-COCO and frozen during training. All the augmentation are the same as those in DETR (Carion et al., 2020). All experiments are conducted on 8 A40 GPUs with a batch size of 16.

## 4. Experimental Results

We comprehensively compare our UAHOI with the recently leading approaches in two representative human-object

**Table 1. Comparison of detection performance on the HICO-DET (Chao et al., 2018) and V-COCO (Gupta and Malik, 2015) test sets, using ResNet50 backbone. The best performance is emphasized in bold.**

Method	Backbone	HICO-DET						V-COCO	
		Default Setup			Known Objects Setup			AP <sup>S1</sup> <sub>role</sub>	AP <sup>S2</sup> <sub>role</sub>
		Full	Rare	Non-rare	Full	Rare	Non-rare		
HO-RCNN (Chao et al., 2018)	CaffeNet	7.81	5.37	8.54	10.41	8.94	10.85	-	-
InteractNet (Gkioxari et al., 2018)	ResNet-50-FPN	9.94	7.16	10.77	-	-	-	40.0	-
GPNN (Qi et al., 2018)	ResNet-101	13.11	9.34	14.23	-	-	-	44.0	-
iCAN (Gao et al., 2018)	ResNet-50	14.84	10.45	16.15	16.26	11.33	17.73	45.3	52.4
TIN (Li et al., 2019)	ResNet-50	17.03	13.42	18.11	19.17	15.51	20.26	47.8	54.2
Gupta et al (Gupta et al., 2019)	ResNet-152	17.18	12.17	18.68	-	-	-	-	-
VSGNet (Ulutan et al., 2020)	ResNet-152	19.80	16.05	20.91	-	-	-	51.8	57.0
DJ-RN (Li et al., 2020a)	ResNet-50	21.34	18.53	22.18	23.69	20.64	24.60	-	-
PPDM (Liao et al., 2020)	Hourglass-104	21.94	13.97	24.32	24.81	17.09	27.12	-	-
VCL (Hou et al., 2020)	ResNet-50	23.63	17.21	25.55	25.98	19.12	28.03	48.3	-
ATL (Hou et al., 2021a)	ResNet-50	23.81	17.43	27.42	27.38	22.09	28.96	-	-
DRG (Gao et al., 2020)	ResNet-50-FPN	24.53	19.47	26.04	27.98	23.11	29.43	51.0	-
IDN (Li et al., 2020b)	ResNet-50	24.58	20.33	25.86	27.89	23.64	29.16	53.3	60.3
HOTR (Kim et al., 2021)	ResNet-50	25.10	17.34	27.42	-	-	-	55.2	64.4
FCL (Hou et al., 2021b)	ResNet-50	25.27	20.57	26.67	27.71	22.34	28.93	52.4	-
HOI-Trans (Zou et al., 2021)	ResNet-101	26.61	19.15	28.84	29.13	20.98	31.57	52.9	-
AS-Net (Chen et al., 2021)	ResNet-50	28.87	24.25	30.25	31.74	27.07	33.14	53.9	-
SCG (Zhang et al., 2021b)	ResNet-50-FPN	29.26	24.61	30.65	32.87	27.89	34.35	54.2	60.9
QPIC (Tamura et al., 2021)	ResNet-101	29.90	23.92	31.69	32.38	26.06	34.27	58.8	61.0
MSTR (Kim et al., 2022)	ResNet-50	31.17	25.31	32.92	34.02	28.82	35.57	62.0	65.2
CDN (Zhang et al., 2021a)	ResNet-101	32.07	27.19	33.53	34.79	29.48	36.38	<b>63.9</b>	65.9
UPT (Zhang et al., 2022)	ResNet-101-DC5	32.62	28.62	33.81	36.08	31.41	37.47	61.3	<b>67.1</b>
RLIP (Yuan et al., 2022a)	ResNet-50	32.84	26.85	34.63	-	-	-	61.9	64.2
GEN-VLKT (Liao et al., 2022)	ResNet-50	33.75	29.25	35.10	36.78	32.75	37.99	62.4	64.5
UAHOI	ResNet-50	<b>34.19</b>	<b>31.54</b>	<b>35.27</b>	<b>37.44</b>	<b>34.18</b>	<b>38.65</b>	62.6	66.7

interaction datasets, HICO-DET (Chao et al., 2018) and V-COCO (Gupta and Malik, 2015) in Table 1. Additionally, we provide some qualitative results in Figure 3.

#### 4.1. Results for HICO-DET

**Dataset.** We first assess UAHOI on human-object interaction datasets HICO-DET (Chao et al., 2018). HICO-DET has 47,776 images, with 38,118 for training and 9,658 designated for testing. There are 600 HOI categories (in total) over 117 interactions and 80 object categories. The interactions are further split into 138 Rare and 462 Non-Rare categories. We calculate the mAP scores using two different setups: (i) the Default Setup, where we compute the mAP across all test images; and (ii) the Known Object Setup, where we calculate the Average Precision (AP) for each object separately, only within the subset of images that contain the specified object.

**Evaluation Metric.** Following the standard evaluation protocols (Qi et al., 2018; Kim et al., 2021), we adopt mean Average Precision (mAP) as the primary metric for accessing model performance.

**Comparison with State-of-the-Art Methods** We first conduct experiments on HICO-DET (Chao et al., 2018) with ResNet-50 as the backbone to verify the effectiveness of the proposed method, and report results in Table 1. Compared to most transformer-based single-decoder works HOITrans (Zou et al.,

2021) and QPIC (Tamura et al., 2021), Our UAHOI achieves better performance, which validates the effectiveness of adopting multi-decoders for detecting more accurate Human-Object Interaction pairs. Compared to RLIP (Yuan et al., 2022a) which introduce language as additional cues for more accurate HOI detection, our method attains improvements from 32.84 mAP to 34.19 mAP for full evaluation under default setting. Even when comparing to the state-of-the-art method GEN-VLKT (Liao et al., 2022), our UAHOI reaches 34.19/31.54/35.27 mAP on the full/rare/non-rare evaluation under the default setting (The best results are highlighted in bold). Especially, UAHOI significantly promotes mAP from 29.25 to 31.54 for rare evaluation under default setting. These results substantiate our motivation to refine the human/object localization and interaction recognition via uncertainty estimation. For the known objects setting, it could be seen that UAHOI achieves 37.44/34.18/38.65 mAP on the full/rare/non-rare evaluation.

#### 4.2. Results for V-COCO

**Dataset.** We next assess UAHOI on a smaller dataset V-COCO (Gupta and Malik, 2015) which originates from COCO (Lin et al., 2014). V-COCO has 2,533/2,867/4,946 images for training, validation, and testing respectively. It consists of 80 objects identical to those in HICO-DET and 29 action categories in total.

**Evaluation Metric.** We also adopt Average Precision (AP) to report performance and compute it under two scenarios to address the challenge of objects missing due to occlusion. We denote these two scenarios with the subscripts  $S_{role}^{S1}$  and  $S_{role}^{S2}$ . In scenario  $S_{role}^{S1}$ , when an object is occluded, we predict empty object boxes to consider the detected pair as a match with the corresponding ground truth. In scenario  $S_{role}^{S2}$ , object boxes are automatically considered matched in cases of occlusion, without the need to predict empty boxes.

**Comparison with State-of-the-Art Methods** We next assess UAHOI on V-COCO (Gupta and Malik, 2015) dataset. Table 1 illustrates the results with both Scenario1 and Scenario2. It could be seen that UAHOI outperforms all existing methods without extra knowledge. We outperform state-of-the-art method GEN-VLKT (Liao et al., 2022) by a large margin of 3.2 mAP under Scenario2. In addition, Compared to the methods with extra language knowledge, UAHOI is still competitive.

### 4.3. Qualitative Results

Additional qualitative results are presented in this section. As shown in Fig 3, we use red lines to denote the detected HOI pairs and blue/green boxes to represent human/object. It can be observed that for common interactions such as sitting, riding, lying, reading, etc., UAHOI demonstrates robust performance. Furthermore, when tackling more challenging scenes with an increased number of humans, ranging from 2 to 5 such as (h), (i), (j), UAHOI continues to perform effectively.

### 4.4. Ablation Study

We evaluate the contribution of each component present in our framework. Specifically, we evaluate UAHOI on the task of HICO-DET Chao et al. (2018), with Res-Net 50 backbone.

**Major Components Analysis.** In this section, we conduct experiments for evaluating major components in our UAHOI: Uncertainty-aware Instance Localization and Interaction Refinement. As shown in Table 2, our base model, utilizing a traditional handcrafted threshold, achieved 31.75 mAP. We then modeled the uncertainty of the bounding box and incorporated the proposed localization refinement module, which improved our results from 31.75 mAP to 32.52 mAP. Furthermore, to enhance the model accuracy in predicting complex interactions and prevent the model from discarding uncertain interaction categories due to a fixed threshold, we applied specific regularization to the prediction variance of the interactions. Using such a dynamic threshold, we optimized interaction uncertainty and achieved higher performance, reaching 33.65 mAP. Finally, by simultaneously employing both localization and interaction uncertainty modules, we elevated the results from 31.75 mAP to 33.65 mAP, achieving optimal performance. This validates the effectiveness of our approach in modeling uncertainty on two levels and integrating uncertainty regularization into our optimization objectives.

**Effect of various uncertainty.** Neural networks are theoretically capable of providing estimates of both confidence, known as aleatoric uncertainty, and model-based uncertainty, referred to as epistemic uncertainty. Existing literatures (Gal

**Table 2. Major component analysis on the HICO-DET test set. Results are averaged across three runs.**

Strategy	Full	Rare	Non-Rare
fixed threshold	31.75	29.42	32.50
+ localization refine	32.52	30.48	33.63
+ interaction refine	33.65	31.27	34.88
+ both	<b>34.19</b>	<b>31.54</b>	<b>35.27</b>

**Table 3. The mAP of different uncertainty modeling strategy on the HICO-DET test set.**

Strategy	Full	Rare	Non-Rare
base	32.52	30.48	33.63
+ Additional Classifier	33.86	30.79	34.82
+ MC Dropout 0.5	33.15	33.65	34.79
+ MC Dropout 0.7	33.22	33.71	34.70
+ MC Dropout 0.9	32.97	33.51	34.35
+ Dropout	<b>34.19</b>	<b>31.54</b>	<b>35.27</b>

and Ghahramani, 2016; Zheng and Yang, 2021) employs various strategies to model uncertainty, and we compared our method with two other approaches. The first approach involves an extra classifier. This method adds another classifier to the existing network architecture to predict interactions, commonly referred to as the auxiliary classification head, while the original classifier is termed the primary classification head. Both classifiers provide predictions, and due to the inherent uncertainty of the model, the outputs from both classifiers are often more uncertain in challenging scenarios. Through regularization of both classifiers’ predictions, refinement of interaction predictions is achieved. As shown in the table, this method reached an accuracy of 33.86 mAP. Subsequently, we compared this with Monte Carlo Dropout (MC-Dropout). MC-Dropout (Gal and Ghahramani, 2016; Lakshminarayanan et al., 2017; Ciosek et al., 2019) is used as another means to estimate epistemic uncertainty. We implement different MC-Dropout rates of 0.5, 0.7, and 0.9 instead of the standard dropout. The results indicate that MC-Dropout also enhances performance and is not sensitive to the dropout rate.

**Effect of dropout depth.** According to the experiments presented in the Table 3, our model is not sensitive to changes in the dropout rate. Therefore, in this section, we perform dropout sampling on models with varying depths of Feed-Forward Networks (FFNs), with results shown in the Table 4. Our base model uses a single layer of FFN without employing dropout, achieving a result of 32.52 mAP. After implementing dropout and conducting uncertainty refinement, the score increased to 34.19 mAP. Using two layers of FFN and applying dropout to each layer further enhanced the performance to 34.27 mAP.

**Parameter sensitivity analysis on loss weights.** We conduct sensitivity analysis on the parameters of loss weights to evaluate the sensitivity of UAHOI on HICO-DET test set. As shown in Table 5, we select loss weights  $\lambda_o$  and  $\lambda_a \in \{0.01, 0.1, 0.5, 1.0, 2.0\}$ . When  $\lambda_o$  and  $\lambda_a$  change significantly, the model exhibits a bit sensitive to the assigned weights. However, when the changes in the coefficients are relatively small, the model is insensitive to the weights, and our method has

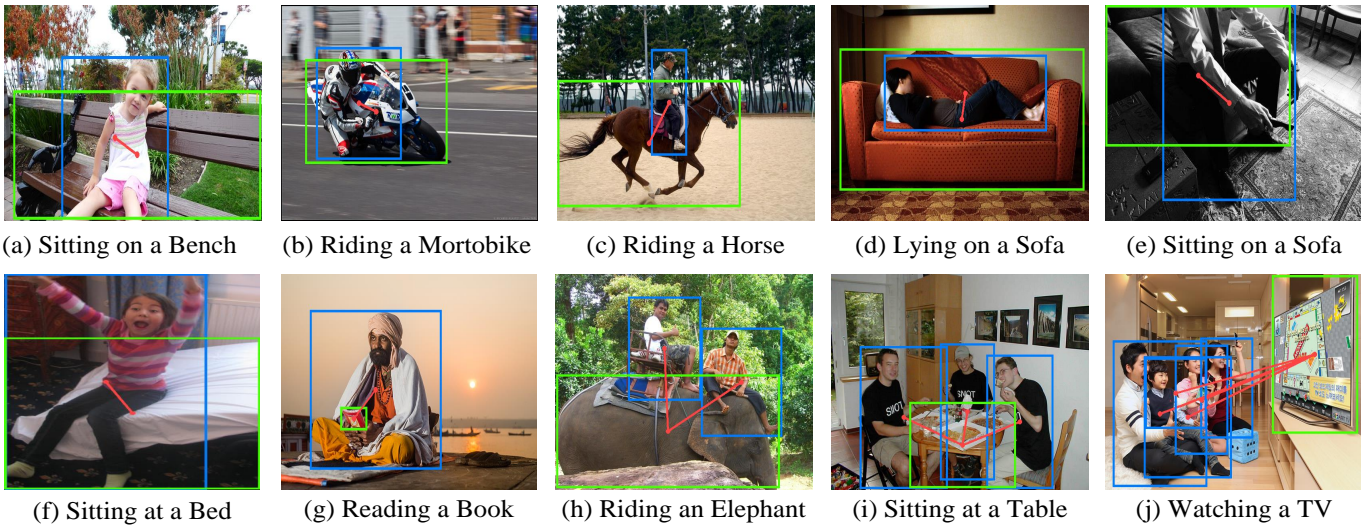


Fig. 3. Visualization results of our UAHOI.

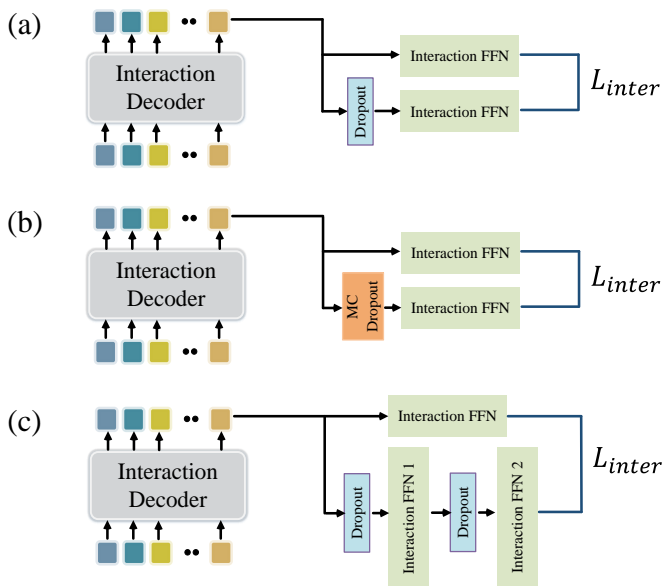


Fig. 4. For a more comprehensive validation of the effects of different uncertainty estimation methods, we further designed our interaction prediction tests by incorporating MC dropout (b), as well as utilizing architectures of Fully Feed-Forward Networks (FFN) with varying depths (c). By adding dropout at different layers, we achieved varying degrees of prediction variance. The results, comparisons, and further analyses are presented in Table 3.

achieved competitive results under various weights.

## 5. Limitations and Future Works

Our architecture consists of a shared transformer encoder along with two separate decoders, making it computationally expensive, which could be detrimental in practical applications. To mitigate this impact, we employ a pre-trained backbone and only fine-tune our network during training to minimize the consumption of computational resources. Additionally, we show failure cases in Fig 5. Due to the presence of complex or overlapping objects, the model is unable to accurately identify all from the visual context.

Table 4. The mAP of different dropout depth on the HICO-DET test set.

Strategy	Full	Rare	Non-Rare
base	32.52	30.48	33.63
with one FFN layer	34.19	31.54	35.27
with two FFN layers	<b>34.27</b>	<b>31.60</b>	<b>35.43</b>

Table 5. Parameter sensitivity analysis on the weight of localization uncertainty loss on HICO-DET test set.

$\lambda_o$	Full	Rare	Non-Rare	$\lambda_a$	Full	Rare	Non-Rare
0.01	32.18	29.45	32.89	0.01	33.65	30.45	34.89
0.1	33.29	30.60	34.06	0.1	33.77	30.86	34.11
0.5	34.09	31.49	35.19	0.5	33.86	31.04	34.55
1.0	<b>34.19</b>	<b>31.54</b>	<b>35.27</b>	1	<b>34.19</b>	<b>31.54</b>	<b>35.27</b>
2.0	32.25	30.22	34.01	2.0	31.95	29.77	33.68

In the future, the impact of dropout uncertainty at different positions (such as in deeper or shallower layers) in the network will be further explored and corresponding improvements will be made. Additionally, the method would be validated on the Scene Graph Generation (SGG) task, which could demonstrate the versatility and effectiveness of uncertainty estimation in other high-level semantic understanding tasks.

## 6. Conclusions

In this paper, we have delved into the application of uncertainty estimation within Human-Object Interaction (HOI) detection, exploring its integration in two key aspects: interaction and detection. For interaction, we utilized dropout not only as a regularization but also as a means for estimating the variance in interaction predictions. This dual-purpose use of dropout allows our model to assess and adapt to the reliability of its interaction classifications dynamically. For detection, we treated the bounding box coordinates as Gaussian-distributed random variables, which enables our system to quantify the uncertainty of object localizations and integrate this information

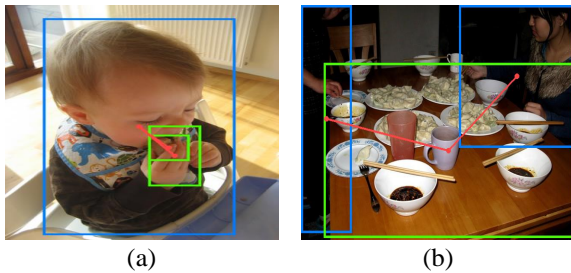


Fig. 5. Visualization results of two failure cases.

into the learning process, thus enhancing prediction confidence and accuracy. Our approach is designed to be orthogonal to existing methods, allowing it to be seamlessly integrated with other techniques, thereby augmenting their effectiveness with robust uncertainty modeling capabilities. This integration capability provides a flexible framework that can be adopted to enhance current HOI detection systems without requiring extensive modifications to existing architectures.

## References

- Amimi, A., Schwarting, W., Soleimany, A., Rus, D., 2020. Deep evidential regression, in: *NeurIPS*.
- Cao, Y., Tang, Q., Su, X., Song, C., You, S., Lu, X., Xu, C., 2023. Detecting any human-object interaction relationship: universal hoi detector with spatial prompt learning on foundation models, in: *NIPS*.
- Carion, N., Massa, F., Synnaeve, G., Usunier, N., Kirillov, A., Zagoruyko, S., 2020. End-to-end object detection with transformers, in: *ECCV*.
- Chao, Y.W., Liu, Y., Liu, X., Zeng, H., Deng, J., 2018. Learning to detect human-object interactions, in: *WACV*.
- Chen, M., Li, L., Wang, W., Quan, R., Yang, Y., 2024a. General and task-oriented video segmentation. *arXiv preprint arXiv:2407.06540*.
- Chen, M., Liao, Y., Liu, S., Chen, Z., Wang, F., Qian, C., 2021. Reformulating hoi detection as adaptive set prediction, in: *CVPR*.
- Chen, M., Zheng, Z., Yang, Y., 2023a. Transferring to real-world layouts: A depth-aware framework for scene adaptation. *arXiv preprint arXiv:2311.12682*.
- Chen, M., Zheng, Z., Yang, Y., 2024b. Pipa++: Towards unification of domain adaptive semantic segmentation via self-supervised learning. *arXiv preprint arXiv:2407.17101*.
- Chen, M., Zheng, Z., Yang, Y., Chua, T.S., 2023b. Pipa: Pixel-and patch-wise self-supervised learning for domain adaptive semantic segmentation, in: *ACM MM*.
- Ciosek, K., Fortuin, V., Tomioka, R., Hofmann, K., Turner, R., 2019. Conservative uncertainty estimation by fitting prior networks, in: *ICLR*.
- Fan, L., Wang, W., Huang, S., Tang, X., Zhu, S.C., 2019. Understanding human gaze communication by spatio-temporal graph reasoning, in: *ICCV*.
- Fang, H.S., Xie, Y., Shao, D., Lu, C., 2021. Dirv: Dense interaction region voting for end-to-end human-object interaction detection, in: *AAAI*.
- Fleuret, F., et al., 2021. Uncertainty reduction for model adaptation in semantic segmentation, in: *CVPR*.
- Frankle, J., Dziugaite, G.K., Roy, D., Carbin, M., 2020. Linear mode connectivity and the lottery ticket hypothesis, in: *ICML*.
- Gal, Y., Ghahramani, Z., 2016. Dropout as a bayesian approximation: Representing model uncertainty in deep learning, in: *ICML*.
- Gal, Y., Hron, J., Kendall, A., 2017. Concrete dropout, in: *NeurIPS*.
- Gao, C., Xu, J., Zou, Y., Huang, J.B., 2020. Drg: Dual relation graph for human-object interaction detection, in: *ECCV*.
- Gao, C., Zou, Y., Huang, J.B., 2018. ican: Instance-centric attention network for human-object interaction detection, in: *BMVC*.
- Gkioxari, G., Girshick, R., Dollár, P., He, K., 2018. Detecting and recognizing human-object interactions, in: *CVPR*.
- Glorot, X., Bengio, Y., 2010. Understanding the difficulty of training deep feed-forward neural networks, in: *Proceedings of the thirteenth international conference on artificial intelligence and statistics, JMLR Workshop and Conference Proceedings*. pp. 249–256.
- Gupta, S., Malik, J., 2015. Visual semantic role labeling. *arXiv preprint arXiv:1505.04474*.
- Gupta, T., Schwing, A., Hoiem, D., 2019. No-frills human-object interaction detection: Factorization, layout encodings, and training techniques, in: *ICCV*.
- Hou, Z., Peng, X., Qiao, Y., Tao, D., 2020. Visual compositional learning for human-object interaction detection, in: *ECCV*.
- Hou, Z., Yu, B., Qiao, Y., Peng, X., Tao, D., 2021a. Affordance transfer learning for human-object interaction detection, in: *CVPR*.
- Hou, Z., Yu, B., Qiao, Y., Peng, X., Tao, D., 2021b. Detecting human-object interaction via fabricated compositional learning, in: *CVPR*.
- Kendall, A., Gal, Y., 2017. What uncertainties do we need in bayesian deep learning for computer vision? *NeurIPS*.
- Kim, B., Choi, T., Kang, J., Kim, H.J., 2020a. Uniondet: Union-level detector towards real-time human-object interaction detection, in: *ECCV*.
- Kim, B., Lee, J., Kang, J., Kim, E.S., Kim, H.J., 2021. Hotr: End-to-end human-object interaction detection with transformers, in: *CVPR*.
- Kim, B., Mun, J., On, K.W., Shin, M., Lee, J., Kim, E.S., 2022. Mstr: Multi-scale transformer for end-to-end human-object interaction detection, in: *CVPR*.
- Kim, D.J., Sun, X., Choi, J., Lin, S., Kweon, I.S., 2020b. Detecting human-object interactions with action co-occurrence priors, in: *ECCV*.
- Lakshminarayanan, B., Pritzel, A., Blundell, C., 2017. Simple and scalable predictive uncertainty estimation using deep ensembles, in: *NeurIPS*.
- Lee, Y., Hwang, J.w., Kim, H.I., Yun, K., Kwon, Y., Bae, Y., Hwang, S.J., 2022. Localization uncertainty estimation for anchor-free object detection, in: *ECCV*.
- Leonardi, R., Ragusa, F., Furnari, A., Farinella, G.M., 2024. Exploiting multi-modal synthetic data for egocentric human-object interaction detection in an industrial scenario. *Computer Vision and Image Understanding* 242, 103984.
- Li, L., Chen, G., Xiao, J., Yang, Y., Wang, C., Chen, L., 2023a. Compositional feature augmentation for unbiased scene graph generation, in: *ICCV*.
- Li, L., Wang, W., Yang, Y., 2023b. Logicseg: Parsing visual semantics with neural logic learning and reasoning, in: *ICCV*.
- Li, L., Wei, J., Wang, W., Yang, Y., 2023c. Neural-logic human-object interaction detection, in: *NeurIPS*.
- Li, L., Xiao, J., Chen, G., Shao, J., Zhuang, Y., Chen, L., 2023d. Zero-shot visual relation detection via composite visual cues from large language models, in: *NIPS*.
- Li, L., Xiao, J., Shi, H., Zhang, H., Yang, Y., Liu, W., Chen, L., 2024. Nicest: Noisy label correction and training for robust scene graph generation. *IEEE Transactions on Pattern Analysis and Machine Intelligence*.
- Li, Y.L., Liu, X., Lu, H., Wang, S., Liu, J., Li, J., Lu, C., 2020a. Detailed 2d-3d joint representation for human-object interaction, in: *CVPR*.
- Li, Y.L., Liu, X., Wu, X., Li, Y., Lu, C., 2020b. Hoi analysis: Integrating and decomposing human-object interaction, in: *NeurIPS*.
- Li, Y.L., Zhou, S., Huang, X., Xu, L., Ma, Z., Fang, H.S., Wang, Y., Lu, C., 2019. Transferable interactiveness knowledge for human-object interaction detection, in: *CVPR*.
- Liang, C., Wang, W., Miao, J., Yang, Y., 2023. Logic-induced diagnostic reasoning for semi-supervised semantic segmentation, in: *ICCV*.
- Liao, Y., Liu, S., Wang, F., Chen, Y., Qian, C., Feng, J., 2020. Ppdm: Parallel point detection and matching for real-time human-object interaction detection, in: *CVPR*.
- Liao, Y., Zhang, A., Lu, M., Wang, Y., Li, X., Liu, S., 2022. Gen-vlkt: Simplify association and enhance interaction understanding for hoi detection, in: *CVPR*.
- Lin, T.Y., Maire, M., Belongie, S., Hays, J., Perona, P., Ramanan, D., Dollár, P., Zitnick, C.L., 2014. Microsoft coco: Common objects in context, in: *ECCV*.
- Liu, W., Anguelov, D., Erhan, D., Szegedy, C., Reed, S., Fu, C.Y., Berg, A.C., 2016. Ssd: Single shot multibox detector, in: *ECCV*.
- Liu, X., Li, Y.L., Wu, X., Tai, Y.W., Lu, C., Tang, C.K., 2022. Interactiveness field in human-object interactions, in: *CVPR*.
- Liu, Y., Chen, Q., Zisserman, A., 2020. Amplifying key cues for human-object-interaction detection, in: *ECCV*.
- Loshchilov, I., Hutter, F., 2017. Decoupled weight decay regularization. *arXiv preprint arXiv:1711.05101*.
- Lu, Z., Li, D., Song, Y.Z., Xiang, T., Hospedales, T.M., 2023. Uncertainty-aware source-free domain adaptive semantic segmentation. *IEEE Transac-*

- tions on Image Processing .
- Miller, D., Nicholson, L., Dayoub, F., Sünderhauf, N., 2018. Dropout sampling for robust object detection in open-set conditions, in: ICRA.
- Miller, D., Sünderhauf, N., Zhang, H., Hall, D., Dayoub, F., 2019. Benchmarking sampling-based probabilistic object detectors., in: CVPR Workshops.
- Ni, Z., Mascaró, E.V., Ahn, H., Lee, D., 2023. Human-object interaction prediction in videos through gaze following. *Computer Vision and Image Understanding* 233, 103741.
- Nian, F., Li, T., Wang, Y., Wu, X., Ni, B., Xu, C., 2017. Learning explicit video attributes from mid-level representation for video captioning. *Computer Vision and Image Understanding* 163, 126–138.
- Ozbulak, U., Vandersmissen, B., Jalalvand, A., Couckuyt, I., Van Messem, A., De Neve, W., 2021. Investigating the significance of adversarial attacks and their relation to interpretability for radar-based human activity recognition systems. *Computer Vision and Image Understanding* 202, 103111.
- Qi, S., Wang, W., Jia, B., Shen, J., Zhu, S.C., 2018. Learning human-object interactions by graph parsing neural networks, in: ECCV.
- Rao, Q., Yu, X., Li, G., Zhu, L., 2024. Cmgnet: Collaborative multi-modal graph network for video captioning. *Computer Vision and Image Understanding* 238, 103864.
- Sensoy, M., Kaplan, L., Kandemir, M., 2018. Evidential deep learning to quantify classification uncertainty, in: NeurIPS.
- Shen, L., Yeung, S., Hoffman, J., Mori, G., Fei-Fei, L., 2018. Scaling human-object interaction recognition through zero-shot learning, in: WACV.
- Srivastava, N., Hinton, G., Krizhevsky, A., Sutskever, I., Salakhutdinov, R., 2014. Dropout: a simple way to prevent neural networks from overfitting. *The journal of machine learning research* 15, 1929–1958.
- Tamura, M., Ohashi, H., Yoshinaga, T., 2021. Qpic: Query-based pairwise human-object interaction detection with image-wide contextual information, in: CVPR.
- Ulutun, O., Iftexhar, A., Manjunath, B.S., 2020. Vsgnet: Spatial attention network for detecting human object interactions using graph convolutions, in: CVPR.
- Vyas, A., Jammalamadaka, N., Zhu, X., Das, D., Kaul, B., Willke, T.L., 2018. Out-of-distribution detection using an ensemble of self supervised leave-out classifiers, in: ECCV.
- Wan, B., Zhou, D., Liu, Y., Li, R., He, X., 2019. Pose-aware multi-level feature network for human object interaction detection, in: ICCV.
- Wang, H., Zheng, W.s., Yingbiao, L., 2020a. Contextual heterogeneous graph network for human-object interaction detection, in: ECCV.
- Wang, T., Yang, T., Danelljan, M., Khan, F.S., Zhang, X., Sun, J., 2020b. Learning human-object interaction detection using interaction points, in: CVPR.
- Wang, W., Yang, Y., Pan, Y., 2024. Visual knowledge in the big model era: Retrospect and prospect. *arXiv preprint arXiv:2404.04308* .
- Wang, W., Zhang, Z., Qi, S., Shen, J., Pang, Y., Shao, L., 2019. Learning compositional neural information fusion for human parsing, in: ICCV.
- Wu, Q., Teney, D., Wang, P., Shen, C., Dick, A., Van Den Hengel, A., 2017. Visual question answering: A survey of methods and datasets. *Computer Vision and Image Understanding* 163, 21–40.
- Xu, B., Wong, Y., Li, J., Zhao, Q., Kankanhalli, M.S., 2019. Learning to detect human-object interactions with knowledge, in: CVPR.
- Yuan, H., Jiang, J., Albanie, S., Feng, T., Huang, Z., Ni, D., Tang, M., 2022a. Rlip: Relational language-image pre-training for human-object interaction detection, in: NeurIPS.
- Yuan, H., Wang, M., Ni, D., Xu, L., 2022b. Detecting human-object interactions with object-guided cross-modal calibrated semantics, in: AAAI.
- Zhang, A., Liao, Y., Liu, S., Lu, M., Wang, Y., Gao, C., Li, X., 2021a. Mining the benefits of two-stage and one-stage hoi detection, in: NeurIPS.
- Zhang, F.Z., Campbell, D., Gould, S., 2021b. Spatially conditioned graphs for detecting human-object interactions, in: ICCV.
- Zhang, F.Z., Campbell, D., Gould, S., 2022. Efficient two-stage detection of human-object interactions with a novel unary-pairwise transformer, in: CVPR.
- Zheng, Z., Yang, Y., 2021. Rectifying pseudo label learning via uncertainty estimation for domain adaptive semantic segmentation. *International Journal of Computer Vision* 129, 1106–1120.
- Zhong, X., Ding, C., Li, Z., Huang, S., 2022. Towards hard-positive query mining for detr-based human-object interaction detection, in: ECCV.
- Zhou, D., Liu, Z., Wang, J., Wang, L., Hu, T., Ding, E., Wang, J., 2022. Human-object interaction detection via disentangled transformer, in: CVPR.
- Zhou, P., Chi, M., 2019. Relation parsing neural network for human-object interaction detection, in: ICCV.
- Zhou, T., Qi, S., Wang, W., Shen, J., Zhu, S.C., 2021. Cascaded parsing of human-object interaction recognition. *IEEE TPAMI* 44, 2827–2840.
- Zhou, T., Wang, W., Qi, S., Ling, H., Shen, J., 2020. Cascaded human-object interaction recognition, in: CVPR.
- Zou, C., Wang, B., Hu, Y., Liu, J., Wu, Q., Zhao, Y., Li, B., Zhang, C., Zhang, C., Wei, Y., et al., 2021. End-to-end human object interaction detection with hoi transformer, in: CVPR.